

# X-ray Galaxies: A Chandra Legacy

Q. Daniel Wang<sup>1</sup>

## ABSTRACT

This presentation reviews Chandra’s major contribution to the understanding of nearby galaxies. After a brief summary on significant advances in characterizing various types of discrete X-ray sources, the presentation focuses on the global hot gas in and around galaxies, especially normal ones like our own. The hot gas is a product of stellar and AGN feedback — the least understood part in theories of galaxy formation and evolution. Chandra observations have led to the first characterization of the spatial, thermal, chemical, and kinetic properties of the gas in our Galaxy. The gas is concentrated around the Galactic bulge and disk on scales of a few kpc. The column density of chemically-enriched hot gas on larger scales is at least an order magnitude smaller, indicating that it may not account for the bulk of the missing baryon matter predicted for the Galactic halo according to the standard cosmology. Similar results have also been obtained for other nearby galaxies. The X-ray emission from hot gas is well correlated with the star formation rate and stellar mass, indicating that the heating is primarily due to the stellar feedback. However, the observed X-ray luminosity of the gas is typically less than a few percent of the feedback energy. Thus the bulk of the feedback (including injected heavy elements) is likely lost in galaxy-wide outflows. The results are compared with simulations of the feedback to infer its dynamics and interplay with the circum-galactic medium, hence the evolution of galaxies.

## 1. Introduction

X-ray observations are playing an increasingly important role in the study of galaxies. With its arcsecond spatial resolution, *Chandra* in particular has made a significant impact on our understanding of discrete X-ray source populations, which mostly represent various stellar end-products [e.g., low- and high-mass X-ray binaries (LMXBs and HMXBs) and supernova remnants (SNRs)] as well as active galactic nuclei (AGNs). The resolution also allows for a clean excision of such sources from the data so low-surface brightness emission (e.g. from diffuse hot gas) can be mapped out. An under-appreciated aspect of *Chandra* is its spectroscopic capability in the study of diffuse hot gas when the low- and high-energy grating instruments are used. Although the sensitivities of the instruments are quite limited, the existing observations of a dozen or so bright objects (AGNs and LMXBs) have yielded data of high enough quality for unprecedented X-ray absorption line spectroscopic measurements of the global hot gas in and around our Galaxy. Useful constraints have also been obtained on the overall content of hot gas around galaxies within certain impact distances of the sight lines toward the AGNs. These measurements, compared with physical models and simulations of the hot gas, are shedding important insights on its relationship to the feedback from stars and AGNs. These aspects of the *Chandra*’s legacy are reviewed in the following.

---

<sup>1</sup>Department of Astronomy, University of Massachusetts, Amherst, USA

## 2. Discrete Sources

The overall X-ray luminosity of a galaxy (except for a giant elliptical) is usually dominated by HMXBs and/or LMXBs. The luminosity functions of HMXBs and LMXBs are linearly scaled with the star formation rate and the stellar mass of a galaxy and are universal to an accuracy better than  $\sim 50\%$  and  $30\%$ , respectively (1; 2). The differential power law slope of the function for HMXBs is  $\approx 1.6$  over a broad range of  $\log(L_x) \sim 35.5 - 40.5$ , where  $L_x$  is the luminosity in the 0.5-2 keV band. Particularly interesting are a large number of non-AGN (hyper)ultraluminous X-ray sources with  $\log(L_x)$  in the range of  $\sim 39.5 - 41.5$  and observed typically in active star forming galaxies, suggesting the presence of either so-called intermediate-mass black holes ( $10 \lesssim M_{BH} \lesssim 10^5$ ) or sources apparently radiating well above the Eddington limit. The luminosity function shape for LMXBs is a bit more complicated, having a slope of  $\approx 1$  at  $\log(L_x) \lesssim 37.5$ , steepening gradually at higher luminosities and cutting off abruptly at  $\log(L_x) \sim 39.0 - 39.5$ . Furthermore, the frequency of LMXBs per stellar mass is substantially higher in globular clusters than in galaxy field (e.g., (3)). This is attributed to the formation of LMXBs via close stellar encounters, which has also been proposed to account for an enhanced number of LMXBs in the dense inner bulge of M 31 (4). But it is not yet clear as to what fraction of field LMXBs was formed dynamically (e.g., (5; 6)).

For the study of diffuse hot gas, it is important to minimize the confusion from point-like source contributions. A source detection limit at least down to  $\log(L_x) \sim 37$  is highly desirable, which can be achieved with a *Chandra* observation of a reasonably deep exposure for nearby galaxies ( $D \lesssim 20$  Mpc). The residual contribution from fainter HMXBs and LMXBs can then be estimated from their correlation with the star formation rate and stellar mass and subtracted from the data with little uncertainty. However, one still needs to be careful with Poisson fluctuations of sources just below the detection limit. Such fluctuations may significantly affect the reliability of X-ray morphological analysis of a galaxy.

In addition to the subtraction of relatively bright X-ray binaries, one also needs to account for a significant (even dominant) stellar contribution from cataclysmic variables and coronally active stars, which are numerous, though individually faint. Very deep *Chandra* imaging of a region toward the Galactic bulge (7) has resolved out more than 80% of the background emission at energies of 6-7 keV, where the observed prominent Fe 6.7-keV line was thought as the evidence for the presence of diffuse hot plasma at  $T \sim 10^8$  K. This high-energy background emission is now shown to be entirely consistent with this collective stellar contribution in the Galactic bulge/ridge. It should be noted, however, that the resolved fraction is much smaller at lower energies ( $\sim 50\%$  at  $\lesssim 4$  keV), which may be considered as an indication for the presence of diffuse hot gas at much lower temperatures. The stellar contribution is unresolved for external galaxies, even nearby ones. Fortunately, the average X-ray spectrum and specific luminosity (per stellar mass) of the contribution have been calibrated, based on the *Chandra* observations of M32, which is too light to hold significant amount of diffuse hot gas), together with the direct detection of stellar X-ray sources in the solar neighborhood (8). The contribution can be readily included in a spectral analysis of the “diffuse” X-ray emission of a galaxy. In an imaging analysis, one may subtract the contribution scaled according to the stellar mass distribution (e.g., traced by the near-IR K-band intensity of a galaxy).

## 3. Global hot gas in and around our Galaxy

The properties of the global hot gas on scales comparable to the size of the Galaxy remained largely unknown until recently. Before *Chandra*, we did have various broad-band X-ray emission surveys of the sky such as the one made by *ROSAT* in the 0.1-2.4 keV range, which is sensitive to the hot gas (9). But such

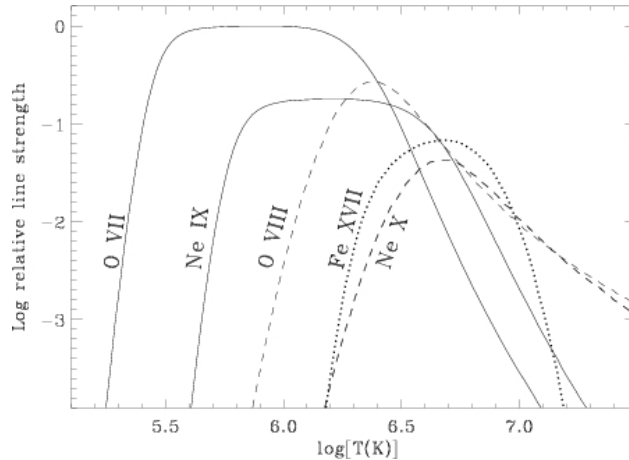


Fig. 1.— Relative line strength (ionization fraction times oscillation strength) of the  $K\alpha$  lines of key species that trace gas in the temperature range of  $10^{5.5} - 10^{6.5}$  K (21).

a survey alone cannot be used to directly determine the origin of the X-ray emission, which carries little distance information. The interpretation of the emission depends sensitively on the assumed cool (X-ray-absorbing) and hot gas distributions. Spectroscopic information on the X-ray emission has been obtained from rocket experiments (10) and more recently from *Suzaku* observations, but only for a number of sample regions (e.g., (11)). There are also large uncertainties in the contributions from faint discrete sources and other irrelevant phenomena such as solar wind charge exchange (SWCX) to the emission.

A breakthrough for the study of the global hot gas has been made from the use of the X-ray absorption line spectroscopy (e.g., (12; 13; 14; 15; 16; 17; 18; 19; 20)). While absorption line spectroscopy is commonly used in optical and UV studies of the interstellar medium (ISM), this technique became feasible in the soft X-ray regime only with grating spectra from *Chandra* and *XMM-Newton*. Unlike the emission, which is sensitive to the density structure, absorption lines produced by ions such as O VII, O VIII, and Ne IX (Fig. 1) directly probe their column densities, which are proportional to the mass of the hot gas. The relative strengths of such absorption lines give direct diagnostics of the thermal, chemical and/or kinetic properties of the hot gas. Although the absorption lines are rarely resolved in the spectra (with a resolution of  $\sim 400 - 500 \text{ km s}^{-1}$  FWHM), the velocity dispersion of the hot gas can be derived from the relative line saturation of different transitions of same ion species (e.g., O VII  $K\alpha$  vs.  $K\beta$ ). Because the K-shell transitions of carbon through iron are all in the X-ray regime, the same technique can be used to study the ISM in essentially all phases (cold, warm, and hot) and forms (atomic, molecular, and dust grain; (16)). Furthermore, the measurements are insensitive to the photo-electric absorption by the cool ISM ( $kT \lesssim 10^4$  K) and to the SWCX. Therefore, the X-ray absorption line spectroscopy allows us to probe the global ISM unbiasedly along a sight line. The effectiveness of the technique can be further enhanced when multiple sight lines are analyzed jointly (e.g., (18)) and/or emission data are included (e.g., (19)). We can then infer differential properties of hot gas between sight lines of different depths or directions and/or estimate the pathlength and density of the hot gas. The application of this X-ray tomography, though only to a very limited number of sight lines so far, has led to the first characterization of the global hot gas:

- The spatial distribution of the gas at the solar neighborhood can be characterized by a thick Galactic disk with a density scale height of  $\sim 2$  kpc (e.g., (15; 17; 20)), comparable to those measured for O VI

(from far-UV absorption line observations) and free electrons (from pulsar dispersion measures). The density is enhanced toward the inner region of the Galaxy, indicating the presence of a Galactic bulge component of the hot gas (15; 16; 18). A temperature increase is also observed from the disk ( $\sim 10^{6.2}$  K) to the bulge ( $\sim 10^{6.4}$  K; e.g., (15; 16; 17; 18; 20)).

- The velocity dispersion increases from  $\sim 60 \text{ km s}^{-1}$  at the solar neighborhood to  $\sim 300 \text{ km s}^{-1}$  toward the inner region of the Galaxy (with 90% uncertainties up to  $\sim 40\%$ ; e.g., (16; 17)), indicating a significant nonthermal (e.g., turbulent) velocity contribution to the line broadening (cf. the thermal broadening  $\sim 40 \text{ km s}^{-1}$ ).
- The metal abundances (O/Fe, Fe/Ne, and O/Ne) are about solar, although there are lines of evidence for the depletion of O and Fe (by a factor of  $\sim 2$ ) at the solar neighborhood (e.g., (16; 20)), assuming the abundances in (22).
- No evidence is yet found for a large-scale X-ray-absorbing hot circum-galactic medium (CGM) with a 95% upper limit to the O VII column density  $N_{\text{OVII}} \sim 3 \times 10^{15} \text{ cm}^{-2}$  for regions  $\gtrsim 10 \text{ kpc}$  away from the Galactic disk/bulge (19) and  $\sim 1 \times 10^{15} \text{ cm}^{-2}$  for  $\gtrsim 50 \text{ kpc}$  (20). This low column density of the hot CGM or the local hot intragroup medium is consistent with the lack of evidence for enhanced X-ray line absorptions along sight lines near the major axis of the Local Group (23).

This basic characterization demonstrates the potential of using the X-ray tomography to greatly advance our understanding of the global hot gas in and around the Galaxy.

#### 4. Global hot gas in and around other galaxies

The X-ray absorption line spectroscopy can also be used to probe the hot CGM around other galaxies. Yao et al. have recently studied the hot CGM along the sight lines toward luminous AGNs (24). As an example, Fig. 2 shows a *Chandra* grating spectrum of PKS 2155-304. No absorption line is apparent at the redshifts of the three groups of galaxies with the impact distances smaller than 500 kpc of the sight line (in particular, the group at the highest redshift contains two galaxies brighter than  $L_*$ ). The same is true when the spectrum is folded according to the redshifts of the individual groups. To increase the counting statistics further, Yao et al. have stacked spectra from the *Chandra* grating observations of eight AGNs with such intervening galaxies or groups. No significant absorption is detected for any of these individual systems or in the final stacked spectrum with a total equivalent exposure of about 10 Ms! Upper limits to the mean column densities of various ion species per galaxy or group are then estimated. In particular, they find that  $N_{\text{OVII}} \leq 6 \times 10^{14} \text{ cm}^{-2}$ , consistent with the constraints for the CGM around our Galaxy. They have estimated the total mass contained in the CGM as  $M_{\text{CGM}} \lesssim 0.6 \times (\frac{0.5}{f_{\text{OVII}}}) \times (\frac{0.3A_{\odot}}{A}) \times (\frac{R}{500 \text{ kpc}})^2 \times 10^{11} M_{\odot}$ , where  $f_{\text{OVII}}$ ,  $A$ , and  $R$  are the ionization fraction of O VII, metal abundance, and the radius of the hot CGM, respectively. This is in contrast to the expected baryon mass  $\gtrsim 2 \times 10^{11} M_{\odot}$  for the halo of a Milky Way-type galaxy or a typical galaxy group (25). Thus the bulk of the CGM unlikely resides in such a chemically enriched warm-hot phase at temperatures ranging from  $10^{5.5} - 10^{6.5} \text{ K}$  (Fig. 1 1), which our X-ray absorption line spectroscopy is sensitive to. This conclusion has strong implications for understanding the accumulated effect of the stellar and AGN feedback on the galactic ecosystem (see the discussion section).

To study the effect of ongoing stellar and AGN feedback, one can map out diffuse X-ray emission from hot gas in and around nearby galaxies of various masses and star formation rates. Much attention has been paid to the feedback in starburst and massive elliptical galaxies, which are relatively bright in diffuse X-ray

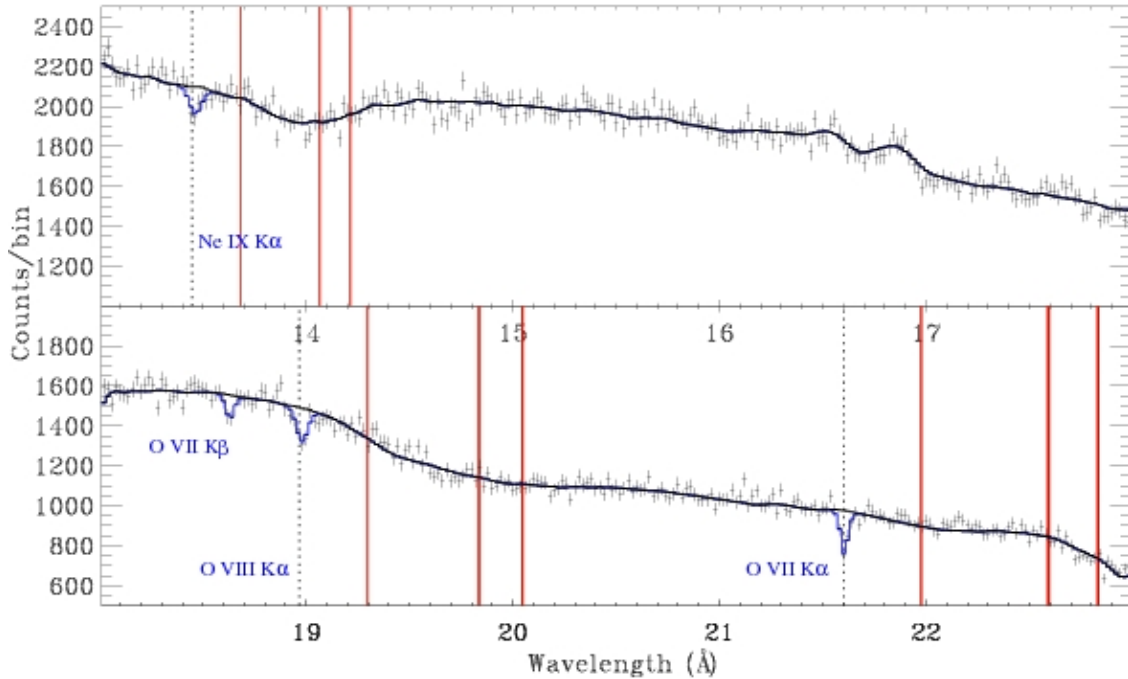


Fig. 2.— Part of the *Chandra* grating spectrum of PKS 2155-304 with a total exposure of 1 Ms. Various absorption lines (marked in blue) are detected and are produced by hot gas in and around the Galaxy (zero redshift). The red-shaded regions enclose spectral ranges of the same lines for three red-shifted groups of galaxies located within the 500 kpc impact distance of the AGN sight line.

emission. *Chandra* observations have shown convincingly that the AGN feedback is important in shaping the morphology and thermal evolution of hot gas in massive elliptical galaxies, particularly those at centers of galaxy groups and clusters ((26) and references therein). The asymmetry in the global diffuse X-ray morphology is correlated with radio and X-ray luminosities of AGNs in elliptical galaxies, even in rather X-ray-faint ones (27). This calls into question the hydrostatic assumption commonly used in order to infer the gravitational mass distribution in such galaxies. Nevertheless, the hydrostatic assumption may hold approximately for hot gas around the central supermassive black holes (SMBHs), if they are in a sufficiently quiescent state. The SMBH masses may then be measured from spatially resolved X-ray spectroscopy of the hot gas. Humphrey et al. have made such mass measurements for four SMBHs with *Chandra* data (28). Three of them already have mass determinations from the kinematics of either stars or a central gas disk. It is encouraging to find a good agreement between the measurements using the different methods. From this agreement, they further infer that no more than  $\sim 10\% - 20\%$  of the ISM pressure around the SMBHs should be nonthermal.

The feedback in nuclear starburst galaxies is manifested in the so-called galactic superwinds driven by the mechanical energy injection from fast stellar winds and supernovae (SNe) of massive stars (e.g., (29; 30; 31)). The observed soft X-ray emission from a superwind typically has an elongated morphology along the minor axis of such a galaxy and is correlated well with extraplanar  $H\alpha$ -emitting features. This indicates that the detected hot gas arises primarily from the interaction between the superwind and cool gas. The superwind itself, believed to be very hot and low in density, is much difficult to detect. From a detailed comparison between *Chandra* data and hydrodynamic simulations, Strickland & Heckman infer that

the superwind of M82 has a mean temperature of  $3 - 8 \times 10^7$  K and a mass outflowing rate of  $\sim 2 M_{\odot} \text{ yr}^{-1}$  (31). Such energetic superwinds with little radiative energy loss must have profound effects on the large-scale CGM (e.g., (30)).

Recent X-ray observations have further shown the importance of the feedback in understanding even “normal” intermediate-mass galaxies (similar to the Milky Way and M31; e.g., (29; 30; 32; 33; 34; 35; 36; 37; 38; 39; 40)). *Chandra*, in particular, has unambiguously detected diffuse hot gas in and around normal disk galaxies. The total X-ray luminosity of the gas is well correlated with the star formation rate for such galaxies. The diffuse soft X-ray emission is shown to be strongly enhanced in recent star forming regions or spiral arms within an individual galaxy viewed face-on and is only slightly more diffuse than H $\alpha$  emission (e.g., (33; 34)). This narrow appearance of spiral arms in X-ray conflicts the expectation from population synthesis models: the mechanical energy output rate from SNe should be nearly constant over a time period that is up to 10 times longer than the lifetime of massive ionizing stars. This means that SNe in inter-arm regions, where ISM density is generally low, must produce less soft X-ray emission than those in the arms. When disk galaxies are observed in an inclined angle (e.g., Fig. 3), the soft X-ray emission tends to appear as plumes, most likely representing blown-out hot gas heated in recent massive star forming regions and galactic spheroids. The cleanest perspectives of the extraplanar hot gas are obtained from the observations of edge-on disk galaxies such as NGC 891 (29) and NGC 5775 (38). The observed diffuse X-ray emission typically does not extend significantly more than a few kpc away from the galactic disks. A claimed detection of the emission around the edge-on spiral NGC 5746 on larger scales was later proved to be due to an instrumental artifact (41). Complementary observations from *XMM-Newton* and *Suzaku* give consistent results and provide improved spectral information on the hot gas (e.g., (35; 36; 40; 42; 43)). The morphology of the X-ray emission as well as its correlation with the star formation rate clearly shows that the extraplanar hot gas is primarily heated by the stellar feedback. In fact, the cooling of the hot gas accounts for only a small fraction of the expected energy input from massive stars alone (typically no more than a few %).

The best example of mapping out hot gas in a galactic stellar bulge (or spheroid) is the discovery of an apparent hot gas outflow from the M31 bulge (37; 39). This outflow with a 0.5-2 keV luminosity of  $\sim 2 \times 10^{38} \text{ erg s}^{-1}$  is driven apparently by the feedback from evolved stars in form of stellar mass loss and (Type) Ia SNe, because there is no evidence for an AGN or recent massive star formation in the bulge. The bipolar morphology of the truly diffuse soft X-ray emission further indicates that the outflow is probably influenced by the presence of strong vertical magnetic field, same as that observed in the central region of our Galaxy. The spectrum of the emission can be characterized by an optically-thin thermal plasma with a temperature of  $\sim 3 \times 10^6$  K (37; 39; 44). Similar analyses have been carried out so far only for a couple of other early-type galaxies (NGC 3379, (45); NGC 5866, (46)). The faint stellar contribution, which has a significantly different spectral shape from LMXBs’, still needs to be carefully accounted for in the analysis of other galaxies. In any case, it is clear that the diffuse X-ray luminosity accounts for at most a few % of the energy input from Ia SNe alone in a normal early-type galaxy. Where does the missing feedback go?

Another remarkable puzzle about the diffuse hot gas in elliptical galaxies is the apparent low metal abundances. As inferred from X-ray spectral fits, the abundances are typically sub-solar for low- and intermediate-mass galaxies with  $\log(L_x) \lesssim 41$  to about solar for more massive ones (e.g., (47; 48)), substantially less than what are expected from the Ia SN enrichment (see the discussion section). Furthermore, a number of galaxies show a significant iron abundance drop toward their central regions, where the stellar feedback should be the strongest. Examples of this abundance drop include M87 (49), NGC 4472, NGC 5846 (50), and NGC 5044 (51). The drop and the low abundance, if intrinsic, would then indicate that only a small portion of metals produced by Ia SNe is observed; the rest is either expelled or in a state that the

present X-ray data are not sensitive to.

In summary, the following are the key discoveries made with *Chandra* observations of diffuse hot gas in and around normal galaxies:

- The hot gas generally consists of two components: 1) the disk component, which is sensitive to the star formation rate per unit area (e.g., (30; 38; 52; 43)); 2) the bulge component, the amount of which is proportional to the stellar mass. Significant diffuse soft X-ray emission is detected only within  $\sim 10$  kpc of the disk and bulge of a galaxy.
- The gas typically has a mean characteristic temperature of  $\sim 10^{6.3} K$ , although there is evidence for a considerably high temperature component (up to  $\gtrsim 10^7 K$ ) in and around galactic disks with active star formation (34; 38). This high-temperature component may represent a significant galactic hot gaseous outflow. The interaction of this outflow with cool gas (via shocks, dynamic mixing, and/or charge exchanges) is responsible for much of the low-temperature one (e.g., (31; 38)).
- The cooling rate, as inferred from the diffuse X-ray emission, is insignificant, compared to the expected stellar feedback alone. The bulk of the feedback is missing, especially in inter-arm regions and in galactic spheroids.
- The hot CGM seems to have a very low density and may not account for the missing baryon matter expected in individual galactic dark matter halos.

While the above results are generally consistent with those found for our own Galaxy, the studies of nearby galaxies also show intriguing sub-structures in the diffuse hot gas distributions (e.g., the apparent positive radial temperature and metal abundance gradients in elliptical galaxies).

## 5. Discussion

As shown above, the diffuse soft X-ray emission observed in and around galaxies clearly traces the global hot gas that is heated by the stellar and possibly AGN feedback. By comparing the X-ray observations directly with physical models and/or simulations of the feedback, we may further study its dynamics, which is so far hardly known. The following discussion is concentrated on the modeling of the feedback in galactic spheroids for their relative simplicity. The presence of substantial cool gas and star formation, as in typical disk galaxies, would certainly add complications.

### 5.1. Comparison of feedback models with X-ray observations

The missing feedback problem is particularly acute in so-called low  $L_X/L_K$  spheroid-dominated galaxies. Empirically, the Ia SN rate is  $\approx 0.019 \text{ SN yr}^{-1} 10^{-0.42(B-K)} [L_K/(10^{10} L_{\odot K})]$ , where  $L_K$  is the K-band luminosity of a galaxy (53). Adopting the color index  $B - K \approx 4$  for a typical spheroid, we estimate the total mechanical energy injection from Ia SNe (assuming  $10^{51}$  ergs each) is  $L_{Ia} \approx (1.3 \times 10^{40} \text{ ergs s}^{-1}) [L_K/(10^{10} L_{\odot K})]$ . The mechanical energy release of an AGN can also be estimated empirically (54; 52) as  $L_{AGN} = (1.1 \times 10^{39} \text{ erg s}^{-1}) [L_K/(10^{10} L_{K,\odot})]^2$ . Therefore, averaged over the time, Ia SNe are energetically more important than the AGN in a galactic spheroid with  $L_K \lesssim 10^{11} L_{K,\odot}$ . Furthermore, SN blastwaves provide a natural distributed heating mechanism for hot gas in galactic spheroids (55). Additional

continuous heating is expected from converting the kinetic energy of stellar mass loss from randomly moving evolved stars to the thermal energy. On the other hand, the AGN feedback, likely occurring in bursts with certain preferential directions (e.g., in form of jets), can occasionally result in significant disturbances in global hot gas distributions, as reflected by the asymmetric X-ray morphologies observed in some elliptical galaxies (e.g., (27)). It is not yet clear as to what fraction of the AGN feedback energy is converted into the heating of the hot gas observed. In general, the lack of distributed cool gas in galactic spheroids makes it difficult to convert and release the thermal energy into radiation in wavelength bands other than the X-ray.

Not only the mechanical energy, the gas mass from the stars and Ia SNe, especially heavy elements, is missing as well. The mass injection rate is expected to be  $0.026[L_K/(10^{10}L_{K,\odot})]M_{\odot}\text{ yr}^{-1}$  with a mean iron abundance  $Z_{Fe} \approx Z_{*,Fe} + 4(M_{Fe}/0.7M_{\odot})$ , where  $Z_{*,Fe}$  is the iron abundance of the stars while  $M_{Fe}$  is the iron mass yield per Ia SN (e.g., (53; 56; 57)). The above empirical estimates of the energy and mass feedback rates, which should be accurate within a factor of  $\sim 2$ , are typically a factor of  $\sim 10^2$  greater than what are inferred from the diffuse X-ray emission. Naturally, one would expect that the missing feedback is gone with a wind (outflow), spheroid-wide or even galaxy-wide.

The notion that Ia SNe may drive galactic winds is not new (e.g., (57; 58; 59)). But could such winds explain the diffuse X-ray emission of galactic spheroids? It is easy to construct a 1-D steady-state supersonic wind model, assuming that the specific energy of the feedback (per mass) of a galaxy is large enough to overcome its gravitational bounding and that the CGM pressure (thermal or ram) is negligible (e.g., (60)). This supersonic wind model depends primarily on two feedback parameters: the integrated energy and mass input rates. However, the model in general fails miserably: it predicts a too low luminosity (by a factor of  $\sim 10^2$ ), a too high temperature (a factor of a few), and a too steep radial intensity profile to be consistent with *Chandra* observations of low  $L_X/L_B$  galactic spheroids, in particular those in M31 and M104 (37; 43). Only few very low-mass and gas-poor spheroids, hence very faint in X-ray emission, still seem to be consistent with the 1-D wind model (e.g., (45)).

To compare with the X-ray emission, in fact one needs to account for 3-D effects. X-ray emission is proportional to the emission measure and is thus sensitive to the detailed structure of hot gas in a galactic spheroid. To realistically generate the inhomogeneity in the heating and chemical enrichment processes, Tang & Wang have developed a scheme to embed adaptively selected 1-D SNR seeds in 3-D spheroid-wide simulations of supersonic winds or subsonic outflows (e.g., (55; 61)). These 3-D simulations, reaching a resolution down to adaptively refined scales of a few pc (e.g., Fig. 4a), show several important 3-D effects (60):

- Soft X-ray emission arises primarily from relatively low temperature and low abundance gas shells associated with SN blastwaves. The inhomogeneity in the gas density and temperature substantially alters the spectral shape and leads to artificially lower metal abundances (by a factor of a few) in a spectral fit with a simplistic thermal plasma model.
- Reverse shock-heated SN ejecta, driven by its large buoyancy, quickly reaches a substantially higher outward velocity than the ambient medium. The ejecta is gradually and dynamically mixed with the medium at large galactic radii and is also slowly diluted and cooled by *insitu* mass injection from evolved stars. These processes together naturally result in the observed positive gradient in the average radial iron abundance distribution of the hot gas, even if mass-weighted.
- The average 1-D and 3-D simulations give substantially different radial temperature profiles; the inner temperature gradient in the 3-D simulation is positive, mimicking a “cooling flow”. (Thus the study

of nearby galactic spheroids may provide important insights into the behavior of the intragroup or intracluster gas around central galaxies, for which sporadic AGN energy injections somewhat mimic the SN heating considered here.).

- The inhomogeneity also enhances the diffuse X-ray luminosity by a factor of a few in the supersonic wind case and more in a subsonic outflow. In addition, a subsonic outflow can have a rather flat radial X-ray intensity distribution.
- The dynamics and hence the luminosity of a subsonic flow further depend on the spheroid star formation and feedback history. This dependence, or the resultant luminosity variance, may then explain the observed large dispersion in the X-ray to K-band luminosity ratios of elliptical galaxies.

All considered, subsonic outflows appear to be most consistent with the X-ray observations of diffuse hot gas in typical intermediate-mass galactic spheroids and elliptical galaxies.

## 5.2. The interplay between the feedback and galaxy evolution

Whether a galactic outflow is supersonic or subsonic depends not only on the specific energy of the ongoing feedback, but also on the properties of the CGM, which is a result of the past interplay between the feedback and the accretion of a galaxy or a group of galaxies from the intergalactic medium (IGM). Tang et al. have illustrated how this interplay may work, based on several 1-D hydrodynamic simulations in the context of galaxy formation and evolution (62). They approximate the feedback history as having two distinct phases: (1) an early starburst during the spheroid formation (e.g., as a result of rapid galaxy mergers) and (2) a subsequent long-lasting and slowly declining injection of mass and energy from evolved low-mass stars. An energetic outward blastwave is initiated by the starburst (including the quasar/AGN phase) and is sustained by the long-lasting stellar feedback. Even for a small galactic spheroid such as the one in the Milky Way, this blastwave may heat up the CGM on scales beyond the present virial radius, thus the gas accretion from the IGM into the galactic halo could be largely reduced (see also (63) for similar results from 3-D cosmological structure formation simulations). The long-lasting stellar feedback initially drives a galactic spheroid wind (Fig. 4b). As the mass and energy injection decreases with time, the feedback may evolve into a subsonic and quasi-stable outflow. This feedback/CGM interplay scenario provides a natural explanation to various observed phenomena:

- It solves the missing feedback problem as discussed earlier; the energy is consumed in maintaining the hot CGM and preventing it from fast cooling.
- The very low density of the CGM explains the dearth of the chemically enriched hot gas observed around galaxies; much of the CGM or the intragroup gas has been pushed away to larger scales (see also (64)).
- The predicted high temperature is consistent with observations of the large-scale hot intragroup medium, which seems always higher than  $10^{6.5}$  K (65).
- The cooling of the material ejected early (e.g., during the initial starbursts; (62)) provides a natural mechanism for high-velocity clouds with moderate metal abundances (Fig. 4b). Such clouds may be seen in 21 cm line emission and in various absorption lines (e.g.,  $\text{Ly}\alpha$ , Mg II, Si III; (66; 67; 68)). O VI line absorptions can then arise from either photo-ionization of the clouds or collisional ionization at their interfaces with the pervasive hot CGM.

## 6. Summary

Based on complementary high-resolution imaging and spectroscopic observations from *Chandra*, we have learned a great deal about various high-energy phenomena and processes in galaxies:

- The luminosity functions and their dependence on the stellar mass and star formation rate are nearly universal for essentially all major types of discrete X-ray sources in galaxies.
- A very hot component of the global ISM in the Galaxy has been revealed, and its global spatial, thermal, chemical, and kinetic properties have been characterized.
- Stringent upper limits have been obtained to the contents of the chemically-enriched CGM around our Galaxy and around other galaxies/groups along the sight lines toward several luminous AGNs.
- Detailed structures of the superwinds emanated from starburst galaxies are resolved, tracing strong interplay between the very hot outflowing gas and the presence of cool gas.
- Sporadic energy injections from AGNs are shown to play an important role in shaping the global hot gas in and around elliptical galaxies.
- Truly diffuse hot gas has also been mapped out for a few nearby normal galaxies, indicating that ongoing stellar feedback may play an important role in regulating the galactic eco-systems.

In conclusion, the existing work has demonstrated the power of *Chandra* observations in probing the stellar and AGN feedback and its effect on galaxy evolution as well as inventorying various kinds of high-energy sources in galaxies.

I thank the referee for constructive comments and the organizers of the Chandra’s First Decade of Discovery conference for the invitation to give the talk that this paper is based on and am grateful to my students and collaborators for their contributions to the work described above, particularly Yangsen Yao who helped to produce Figures 1 and 2. The work is partly supported by NASA/CXC under grants G08-9088B and G08-9047A.

## REFERENCES

- Grimm H J, Gilfanov M, and Sunyaev R (2003) *High-mass X-ray binaries as a star formation rate indicator in distant galaxies*, MNRAS, 339, 793-809.
- Gilfanov M (2004) *Low-mass X-ray binaries as a stellar mass indicator for the host galaxy*, MNRAS, 349, 46-168.
- Sarazin C L, et al. (2003) *Low-Mass X-Ray Binaries and Globular Clusters in Early-Type Galaxies*, ApJ, 595..743-759.
- Voss R, and Gilfanov M (2007) *A study of the population of LMXBs in the bulge of M31*, A&A, 468, 49-59.
- White R E III, Sarazin C L, and Kulkarni S R (2002) *X-Ray Binaries and Globular Clusters in Elliptical Galaxies*, ApJL, 571, 23-26.

- Voss R, et al. (2009) *Luminosity Functions of LMXBs in Centaurus a: Globular Clusters Versus the Field*, ApJ, 701, 471-480.
- Revnivtsev M, Sazonov S, Churazov E, Forman W, Vikhlinin A and Sunyaev R (2009) *Discrete sources as the origin of the Galactic X-ray ridge emission*, Nature, 458, 1142-1144.
- Revnivtsev M, Churazov E, Sazonov S, Forman W, and Jones, C (2008) *Universal X-ray emissivity of the stellar population in early-type galaxies: unresolved X-ray sources in NGC 3379*, A&A, 490, 37-43.
- Snowden S L, et al. (1997) *ROSAT Survey Diffuse X-Ray Background Maps*, ApJ, 485, 125-135.
- McCammon D, et al. (2002) *A High Spectral Resolution Observation of the Soft X-Ray Diffuse Background with Thermal Detectors*, ApJ, 576, 188-203.
- Yoshino T, et al. (2009) *Energy Spectra of the Soft X-Ray Diffuse Emission in Fourteen Fields Observed with Suzaku*, PASJ, 61, 805-823.
- Futamoto K, Kazuhisa M, Yoh T, Ryuichi F, and Noriko Y Y (2004) *Detection of Highly Ionized O and Ne Absorption Lines in the X-Ray Spectrum of 4U 1820-303 in the Globular Cluster NGC 6624*, ApJ, 605, 793-799.
- Wang Q D, et al. (2005) *Warm-Hot Gas in and around the Milky Way: Detection and Implications of O VII Absorption toward LMC X-3*, ApJ, 635, 386-395.
- Williams R, et al. (2005) *Probing the Local Group Medium toward Markarian 421 with Chandra and the Far Ultraviolet Spectroscopic Explorer*, ApJ, 631, 856-867.
- Yao Y, and Wang Q D, (2005) *X-Ray Absorption Line Spectroscopy of the Galactic Hot Interstellar Medium*, ApJ, 624, 751-761.
- Yao Y, and Wang Q D (2006) *X-Ray Absorption Spectroscopy of the Multiphase Interstellar Medium: Oxygen and Neon Abundances*, ApJ, 641, 930-937.
- Yao Y, and Wang Q D (2007) *The Nonisothermality and Extent of Galactic Diffuse Hot Gas toward Markarian 421*, ApJ, 658, 1088-1095.
- Yao Y, and Wang Q D (2007) *The Galactic Central Diffuse X-Ray Enhancement: A Differential Absorption/Emission Analysis*, ApJ, 666, 242-246.
- Yao Y, Nowak M A, Wang Q D, Schulz N S, and Canizares C R (2008) *Limits on Hot Galactic Halo Gas from X-Ray Absorption Lines*, ApJL, 672, 21-24.
- Yao Y, et al. (2009) *X-Ray and Ultraviolet Spectroscopy of Galactic Diffuse Hot Gas Along the Large Magellanic Cloud X-3 Sight Line*, ApJ, 690, 143-153.
- Gnat O, and Sternberg A (2007) *Time-dependent Ionization in Radiatively Cooling Gas*, ApJS, 168, 213-230.
- Anders E, and Grevesse N (1989) *Abundances of the elements - Meteoritic and solar*, Geochim. Cosmochim. Acta, 53, 197-214
- Bregman J N, and Lloyd-Davies E J (2007) *X-Ray Absorption from the Milky Way Halo and the Local Group*, ApJ, 669, 990-1002.

- Yao Y, et al. (2010) The dearth of the chemically enriched warm-hot Circum-galactic medium, Ap J, submitted.
- McGaugh S S, Schombert J M, de Blok W J G, and Zagursky M J (2009) *The Baryon Content of Cosmic Structures*, ApJL, in press (arXiv:0911.2700v1).
- McNamara B R, and Nulsen P E J (2007) *Heating Hot Atmospheres with Active Galactic Nuclei*, ARA&A, 45, 117-175.
- Diehl S, and Statler T S (2008) *The Hot Interstellar Medium of Normal Elliptical Galaxies. II. Morphological Evidence for Active Galactic Nucleus Feedback*, ApJ, 680, 897-910
- Humphrey P J, Buote D A, Brighenti F, Gebhardt K, and Mathews W G (2009) *Hydrostatic Gas Constraints on Supermassive Black Hole Masses: Implications for Hydrostatic Equilibrium and Dynamical Modeling in a Sample of Early-type Galaxies*, ApJ, 703, 1257-1277.
- Strickland D K, Heckman T M, Colbert E J M, Hoopes C G, and Weaver K A (2004) *A High Spatial Resolution X-Ray and H $\alpha$  Study of Hot Gas in the Halos of Star-forming Disk Galaxies. I. Spatial and Spectral Properties of the Diffuse X-Ray Emission*, ApJS, 151, 193-236.
- Strickland D K, Heckman T M, Colbert E J M, Hoopes C G, and Weaver K A (2004) *A High Spatial Resolution X-Ray and H $\alpha$  Study of Hot Gas in the Halos of Star-forming Disk Galaxies. II. Quantifying Supernova Feedback*, ApJ, 606, 829-852.
- Strickland D K, and Heckman T M (2009) *Supernova Feedback Efficiency and Mass Loading in the Starburst and Galactic Superwind Exemplar M82*, ApJ, 697, (2030-2056.
- Wang Q D, Chaves T, and Irwin J A (2003) *Chandra Observation of the Edge-on Galaxy NGC 3556 (M108): Violent Galactic Disk-Halo Interaction Revealed*, ApJ, 598, 969-981.
- Tyler K, Quillen A C, LaPage A, Rieke G H (2003) *Diffuse X-Ray Emission in Spiral Galaxies* ApJ, 610, 213-225.
- Doane N E, Sanders W T, Wilcots E M, and Juda M (2004) *The Origin and Distribution of Diffuse Hot Gas in the Spiral Galaxy NGC 3184* AJ, 128, 2712-2723.
- Tüllmann R, Pietsch W, Rossa J, Breitschwerdt D, and Dettmar R J (2006) *The multi-phase gaseous halos of star-forming late-type galaxies. I. XMM-Newton observations of the hot ionized medium*, A&A, 448, 43-75
- Tllmann R, Breitschwerdt D, Rossa J, Pietsch W, and Dettmar R J (2006) *The multi-phase gaseous halos of star-forming late-type galaxies. II. Statistical analysis of key parameters*, A&A, 457, 779-785.
- Li Z, and Wang Q D (2007) *Chandra Detection of Diffuse Hot Gas in and around the M31 Bulge*, ApJL, 668, 39-42.
- Li J T, Li Z, Wang Q D, Irwin J A, and Rossa J (2008) *Chandra observation of the edge-on spiral NGC 5775: probing the hot galactic disc/halo connection*, MNRAS, 390, 59-70.
- Bogdán Á, and Gilfanov M (2008) *Unresolved emission and ionized gas in the bulge of M31*, MNRAS, 388, 56-66.

- Yamasaki N Y, Sato K, Mitsuishi I, and Ohashi T (2009) *X-Ray Halo around the Spiral Galaxy NGC 4631 Observed with Suzaku*, PASJ, 61, S291-S298.
- Rasmussen J, et al (2009) *Hot Gas Halos Around Disk Galaxies: Confronting Cosmological Simulations with Observations*, ApJ, 697, 79-93.
- Li Z, Wang Q D, Irwin J A, and Chaves T (2006) *An XMM-Newton observation of the massive edge-on Sb galaxy NGC 2613*, MNRAS, 371, 147-156.
- Li Z, Wang Q D, and Hameed S (2007) *Chandra and XMM-Newton detection of large-scale diffuse X-ray emission from the Sombrero galaxy*, MNRAS, 376, 960-976.
- Li Z, Wang Q D, and Wakker B (2007) *M31\* and its circumnuclear environment*, MNRAS, 379, 148-163.
- Trinchieri G, et al (2008) *Discovery of Hot Gas in Outflow in NGC 3379*, ApJ, 688, 1000-1008.
- Li J, Wang Q D, Li Z, and Chen Y (2009) *Dynamic S0 Galaxies: a Case Study of NGC 5866*, MNRAS, 390, 693-704.
- Humphrey P J, and Buote D A (2006) *A Chandra Survey of Early-Type Galaxies. I. Metal Enrichment in the Interstellar Medium*, ApJ, 639, 136-156.
- Ji J, Irwin J A, Athey A, Bregman J N, and Lloyd-Davies E J (2009) *Elemental Abundances in the X-Ray Gas of Early-Type Galaxies with XMM-Newton and Chandra Observations*, ApJ, 696, 2252-2268.
- Gastaldello F, and Molendi S (2002) *Abundance Gradients and the Role of Supernovae in M87*, ApJ, 572, 160-168.
- Buote D A (2000) *Iron Gradients in Cooling Flow Galaxies and Groups*, ApJ, 539, 172-186.
- Buote D A, Lewis A D, Brighenti F, and Mathews W G (2003) *XMM-Newton and Chandra Observations of the Galaxy Group NGC 5044. I. Evidence for Limited Multiphase Hot Gas*, ApJ, 595, 151-166.
- David L P, Jones C, Forman W, Vargas I M, and Nulsen P (2006) *The Hot Gas Content of Low-Luminosity Early-Type Galaxies and the Implications Regarding Supernova Heating and Active Galactic Nucleus Feedback*, ApJ, 653, 207-221.
- Mannucci F, Dell V M, and Panagia N (2006) *The supernova rate per unit mass*, MNRAS, 370, 773-783.
- Best P N, Kaiser C R, Heckman T M, and Kauffmann G (2006) *AGN-controlled cooling in elliptical galaxies*, MNRAS, 368, 67-71.
- Tang S, and Wang Q D (2005) *Supernova Blast Waves in Low-Density Hot Media: A Mechanism for Spatially Distributed Heating*, ApJ, 628, 205-209.
- Knapp G, et al. (1992) *Infrared emission and mass loss from evolved stars in elliptical galaxies*, ApJ, 399, 76-93.
- Ciotti L, D’Ercole A, Pellegrini S, and Renzini A (1991) *Winds, outflows, and inflows in X-ray elliptical galaxies*, ApJ, 376, 380-403.
- Mathews W G, and Baker J C (1971) *Galactic Winds*, ApJ, 170, 241-259.
- Bregman J N (1980) *A wind in the Galaxy*, ApJ, 237, 280-284.

- Tang S, Wang Q D, Mac Low M-M, and Joung M R (2009) *Type-Ia Supernova-driven Galactic Bulge Wind*, MNRAS, 398, 1468-1482.
- Tang S, and Wang Q D (2009) *Scalability of Supernova Remnants Simulations*, MNRAS, 397, 2106-2110.
- Tang S, Wang Q D, Lu Y, and Mo H (2009) *Feedback from galactic stellar bulges and hot gaseous halos of galaxies*, MNRAS, 392, 77-90.
- Kim J-H, Wise J H, and Abel T (2009) *Galaxy Mergers with Adaptive Mesh Refinement: Star Formation and Hot Gas Outflow*, ApJL, 694, 123-127.
- Oppenheimer B D, and Davé R (2008) *Mass, metal, and energy feedback in cosmological simulations*, MNRAS, 387, 577-600.
- Sun M, et al. (2009) *Chandra Studies of the X-Ray Gas Properties of Galaxy Groups*, ApJ, 693, 1142-1172.
- Stocke J T, et al. (2006) *The Galaxy Environment of O VI Absorption Systems*, ApJ, 641, 217-228.
- Wakker B P, and Savage B D (2009) *The Relationship Between Intergalactic H I/O VI and Nearby ( $z \lesssim 0.017$ ) Galaxies*, ApJS, 182, 378-467.
- Shull J M, Jones J R, Danforth C W, and Collins J A (2009) *A Large Reservoir of Ionized Gas in the Galactic Halo: Ionized Silicon in High-velocity and Intermediate-velocity Clouds*, ApJ, 699, 754-767

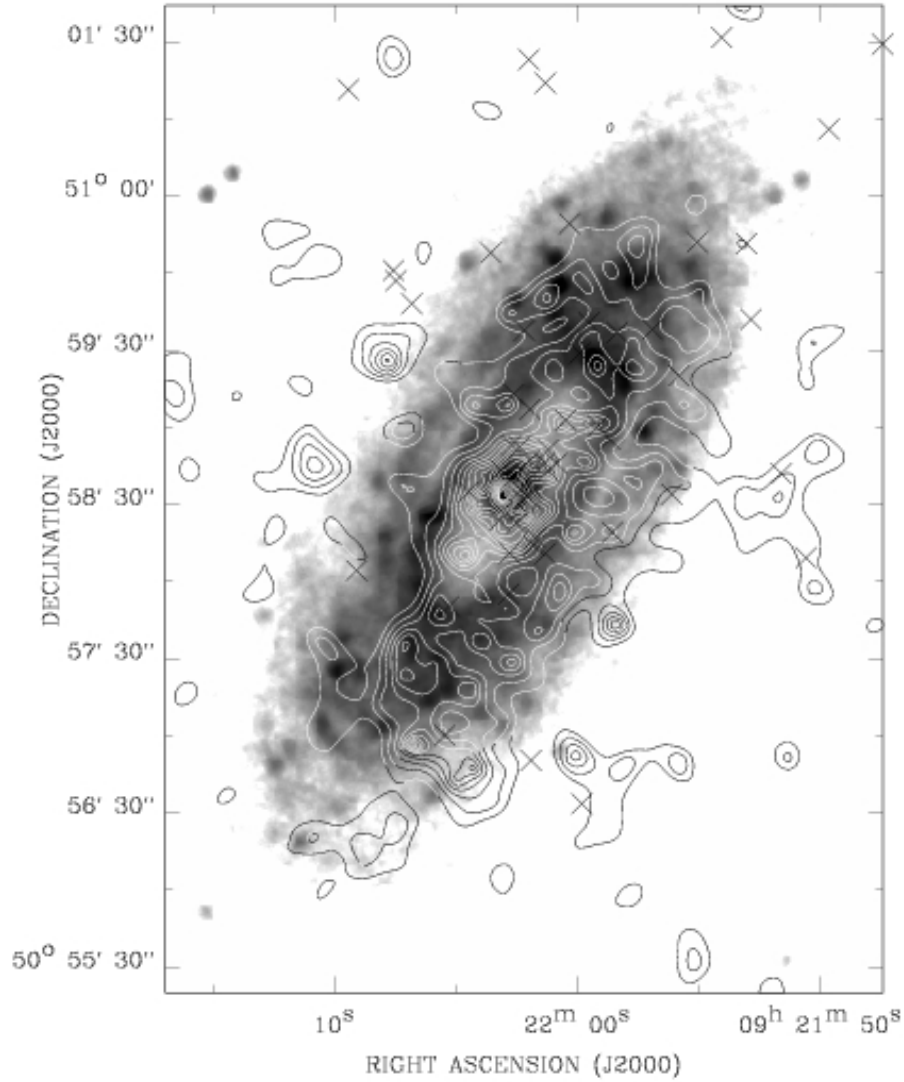


Fig. 3.— *Chandra* diffuse 0.5–1.5 keV intensity contours, overlaid on a *Spitzer* mid-IR image of the Sb galaxy NGC 2841. The one-sided morphology of the diffuse X-ray emission apparently represents outflows of hot gas from the tilted galactic disk with its northeast edge closer to us. The emission from the back side is largely absorbed by the cool gas in the disk. The crosses mark the positions of excised discrete X-ray sources.

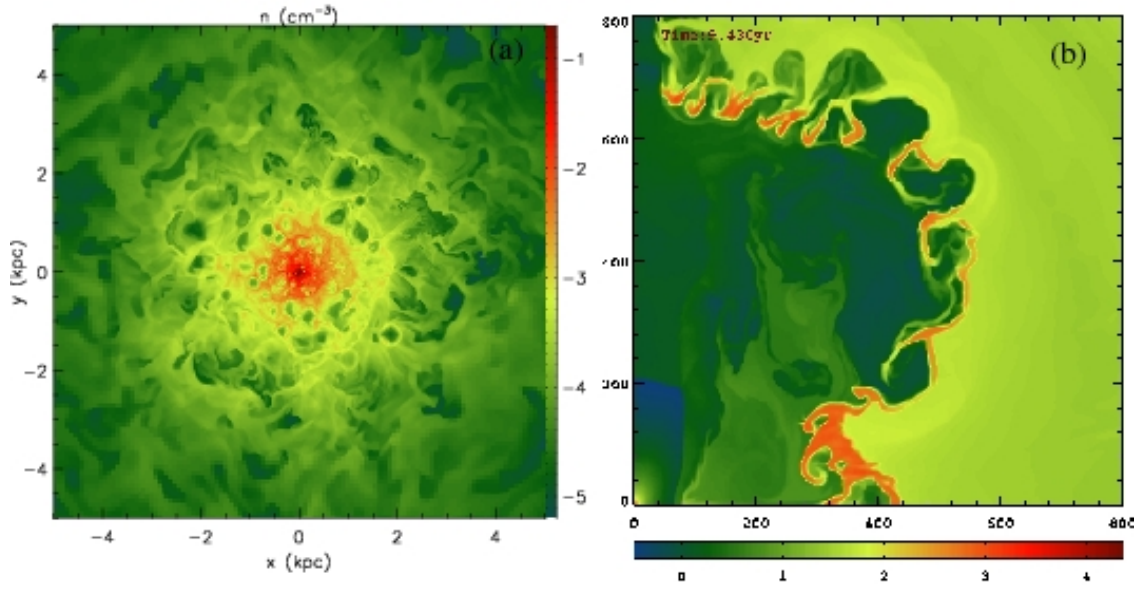


Fig. 4.— Sample snapshots of hydrodynamic simulations of the stellar feedback. **(a)** the 3-D simulated gas density distribution in an M31-like galactic spheroid. The slice is cut near the spheroid center and the units are in  $\text{atoms cm}^{-3}$ , logarithmically. **(b)** Simulated 2-D large-scale gas density distribution in the  $r-z$  plane (in units of kpc). A nearly vertical magnetic field, similar to what is observed in the inter-cloud medium of the Galactic center, is included in the simulation to test its confinement effect on the spheroid wind; a reverse-shock is clearly visible. Also apparent are instabilities at the contact discontinuity between the shocked spheroid wind gas and the ejected materials from the initial starburst. The density is scaled in units of  $M_{\odot} \text{ kpc}^{-3}$ .